2021

Large-Scale Variation in Wave Attenuation of Oyster Reef Living Shorelines and the Influence of Inundation Duration

Rebecca L. Morris

Megan K. La Peyre

Bret M. Webb

Danielle A. Marshall

Donna M. Bilkovic

See next page for additional authors

Original Publication Citation

Large-scale variation in wave attenuation of oyster reef living shorelines and the influence of inundation duration. *Ecological Applications, 31*(6), Article e0238. https://doi.org/10.1002/eap.2382

Authors

Rebecca L. Morris, Megan K. La Peyre, Bret M. Webb, Danielle A. Marshall, Donna M. Bilkovic, Just Cebrian, Giovanna McClenachan, Kelly M. Kibler, Linda J. Walters, David Bushek, Eric L. Sparks, Nigel A. Temple, Joshua Moody, Kory Angstadt, Joshua Goff, Maura Boswell, Paul Sacks, and Stephen E. Swearer

DR. REBECCA LOUISE MORRIS (Orcid ID : 0000-0003-0455-0811)

DR. DAVID BUSHEK (Orcid ID : 0000-0002-0701-4267)

PROF. STEPHEN E. SWEARER (Orcid ID : 0000-0001-6381-9943)

Article type : Articles

Journal: Ecological Applications

Manuscript type: Article

Running head: Oyster reefs and coastal defense

Large-scale variation in wave attenuation of oyster reef living shorelines and the influence of inundation duration

Rebecca L. Morris[1], Megan K. La Peyre[2], Bret M. Webb[3], Danielle A. Marshall[4], Donna M. Bilkovic[5], Just Cebrian[6], Giovanna McClenachan[7,8], Kelly M. Kibler[9], Linda J. Walters[7], David Bushek[10], Eric L. Sparks[11,12], Nigel A. Temple[11], Joshua Moody[13], Kory Angstadt[5], Joshua Goff[14], Maura Boswell[15], Paul Sacks[7], and Stephen E. Swearer[1]

[1]National Centre for Coasts and Climate, School of BioSciences, The University of Melbourne, VIC 3010, Australia; [2]U.S. Geological Survey, Louisiana Cooperative Fish and Wildlife Research Unit, School of Renewable Natural Resources, Louisiana State University Agricultural Center, Baton Rouge, LA 70803, USA; [3]Department of Civil, Coastal & Environmental Engineering, University of

South Alabama, Mobile, AL 36688, USA; [4]School of Renewable Natural Resources, Louisiana State University Agricultural Center, Baton Rouge, LA 70803, USA; [5]Virginia Institute of Marine Science, William & Mary, Gloucester Point, VA 23062, USA; [6]Northern Gulf Institute, Mississippi State University, Stennis Space Center, MS 39529, USA; [7]Department of Biology and National Center for Integrated Coastal Research, University of Central Florida, Orlando, FL 32816, USA; [8]Department of Biological Sciences, Nicholls State University, Thibodaux, LA 70301, USA; [9]Department of Civil, Environmental & Construction Engineering and National Center for Integrated Coastal Research, University of Central Florida, Orlando, FL 32816, USA; [10]Haskin Shellfish Research Laboratory, Rutgers University, Port Norris, NJ 08349, USA; [11]Coastal Research and Extension Center, Mississippi State University, Biloxi, MS 39532, USA; [12]Mississippi-Alabama Sea Grant Consortium, Ocean Springs, MS 39564, USA; [13]Partnership for Delaware Estuary, Wilmington, DE 19801, USA; [14]Dauphin Island Sea Lab, Dauphin Island, AL 36528, USA; [15]Department of Civil and Environmental Engineering, Old Dominion University, Norfolk, VA 23529, USA.

Corresponding Author:
Rebecca Morris, E-mail rebecca.morris@unimelb.edu.au

Manuscript received 22 August 2020; revised 4 January 2021; accepted 4 February 2021; final version received 5 May 2021.

Abstract

One of the paramount goals of oyster reef living shorelines is to achieve sustained and adaptive coastal protection, which requires meeting ecological (i.e., develop a self-sustaining oyster population) and engineering (i.e., provide coastal defense) targets. In a large-scale comparison along the Atlantic and Gulf coasts of the United States, the efficacy of various designs of oyster reef living shorelines at providing wave attenuation was evaluated accounting for the ecological limitations of oysters with regards to inundation duration. A critical threshold for intertidal oyster reef establishment is 50% inundation duration. Living shorelines that spent less than half of the time (< 50%) inundated were not considered suitable habitat for oysters, however, were effective at wave attenuation (68% reduction in wave height). Reefs that experienced > 50% inundation were considered suitable habitat for oysters, but wave attenuation was similar to controls (no reef; ~5% reduction in wave height). Many of the oyster reef living shoreline approaches therefore failed to optimize the ecological and engineering goals. In both inundation regimes, wave transmission decreased with an increasing freeboard (difference between reef crest elevation and water level), supporting its importance in the wave attenuation capacity of oyster reef living shorelines. However, given that the reef crest elevation (and thus freeboard) should be determined by the inundation duration requirements of oysters, research needs to be re-focused on understanding the implications of other reef parameters (e.g. width) for optimising wave attenuation. A broader understanding of the reef characteristics and seascape contexts that result in effective coastal defense by oyster reefs is needed to inform appropriate design and implementation of oyster-based living shorelines globally.

Keywords: coastal management; coastal erosion; nature-based coastal defense; shoreline protection; wave transmission

Introduction

Oyster reefs are highly valued as a fishery resource and as biogenic habitat for a diverse suite of marine species (Grabowski et al. 2012, Cohen and Humphries 2017). Their ecological and socio-economic worth has driven extensive oyster reef restoration, in response to widespread declines in oyster populations (85% functionally extinct; Beck et al. 2011). Recently, there has been increased interest in constructing or restoring oyster reefs for living shoreline applications to stem erosion (Piazza et al. 2005; Bilkovic et al. 2016). Living shorelines are engineered structures primarily composed of natural materials that can be used as an alternative to other “harder” engineered structures, such as seawalls and rock revetments, which are environmentally (Bulleri and Chapman 2010) and economically (Hinkel et al. 2014) costly. Oyster reefs can alter hydrodynamic conditions in estuarine systems through increasing bed friction (Wright et al. 1990, Whitman and Reidenbach 2012, Styles 2015, Kitsikoudis et al. 2020), facilitating wave attenuation (Manis et al. 2015) and accreting sediment on the leeward side of the reef (Salvador de Paiva et al. 2018, Chowdhury et al. 2019). This will become particularly relevant in the future as increased risk of climate change-related erosion and flooding to burgeoning human populations along the coast (Young et al. 2011, Neumann et al. 2015, Meucchi et al. 2020) will result in an increased need for investment in coastal protection infrastructure, and the development of adaptive and sustainable approaches to shoreline protection (Morris et al. 2020).

Traditional coastal defense structures (e.g., seawalls, breakwaters) have usually undergone extensive numerical and physical modelling to identify the important design parameters and their performance under various environmental conditions (e.g. wave heights, water depths). Low crested breakwaters are constructed at or below the water level (i.e., submerged), and can inform wave transmission at oyster reef living shorelines. In low crested breakwaters, wave transmission is most sensitive to the depth of breakwater submergence, the incident wave height, and the crest width (Seabrook and Hall, 1998; van der Meer et al. 2005). Wave transmission increases with increased submergence, increased incident wave height, and decreased crest width (Seabrook and Hall, 1998; van der Meer et al. 2005). Crest width becomes particularly important as submergence increases, whereas freeboard (difference between reef crest elevation and water level) has a larger effect when submergence is reduced (Seabrook and Hall, 1998). Secondarily, the period of the incident wave, the breakwater armour dimensions (in the case of a rubble mound structure), and the breakwater slope have small effects on wave transmission (Seabrook and Hall 1998).

Similar to breakwater construction, the creation of an oyster reef living shoreline begins with the placement of reef substratum such as oyster shell, pre-cast concrete structures, or crushed limestone (Hernandez et al. 2018, Morris et al. 2019a) for oyster colonisation. Physical modelling of the reef substrate agrees with findings from low-crested breakwaters that the freeboard, crest width and incident wave height are key parameters for wave transmission (Allen and Webb 2011, Webb and Allen 2015, Coghlan et al. 2016). This pattern of wave attenuation as a function of water depth in relation to the crest elevation has also been confirmed in field studies (Chauvin 2018, MacDonald 2018, Wiberg et al. 2018, Chowdhury et al. 2019, Zhu et al. 2020, Spiering et al. in revision). While this research has clearly shown that a smaller submergence results in greater wave attenuation by oyster reefs, these findings do not take into account oyster habitat requirements, a necessary consideration for the appropriate application of oyster reef-based living shorelines.

Unlike static structures, the vertical reef building capacity of oysters makes them a candidate for creating dynamic structures (Mitchell and Bilkovic 2019). Oyster reefs exhibit a natural resilience and adaptive capacity to recover quickly from major storm events (Livingston et al. 1999) and are capable of accreting at a rate necessary to maintain elevation in areas facing sea-level rise (Rodriguez et al. 2014) or local subsidence (Casas et al. 2015). A key variable that affects the recruitment, survival, and growth of oyster reefs is the duration of inundation (Table 1), which is a function of the absolute elevation of the reef and the tidal range. The lower elevation threshold of intertidal oysters is commonly determined by increased biofouling, predation, competition, or sedimentation in the subtidal (Fodrie et al. 2014, Solomon et al. 2014), whereas the maximum elevation of oysters in the intertidal is driven by availability of filter feeding time and exposure to extreme temperature stress. The optimum inundation duration, therefore, is a trade-off among these limiting factors. The inundation duration has been reasonably well-studied for the eastern oyster (*Crassostrea virginica*) in some locations along the east coast of the United States (Table 1). This species is generally found at 60-80% inundation, with lower and upper boundaries at 50% and 95% inundation, respectively (Fodrie et al. 2014; Byers et al. 2015; Ridge et al. 2014, 2017; Solomon et al. 2014; Marshall and La Peyre, 2020; Table 1). Thus, for intertidal oysters, constructing a reef base at an elevation that spends more than 50% of the time inundated is critical for oyster establishment. Consequently, there is a dichotomy between the reef elevation for optimal engineering design and habitat provisioning for oysters.

As efforts to characterise wave attenuation by oyster reef living shorelines are growing, the aim of this paper is to assess whether observed trends in oyster reef wave attenuation apply across different environments and reef types using data across a large spatial scale. Further, we consider wave transmission alongside the ecological limitations for oysters to characterize the expected balance between effective wave attenuation and likelihood of reef persistence. Wave attenuation was measured at 15 oyster reef living shoreline-control pairs in five locations (New Jersey/Delaware, Virginia, Florida, Alabama and Louisiana) along the Atlantic and Gulf coasts of the United States. At each location we assessed the effects of oyster reef living shorelines compared to controls (no reef) on wave attenuation relative to the inundation duration of the reef. It was predicted that: (1) wave transmission would be greater at oyster reefs with an inundation duration of > 50% compared with < 50%; (2) for oyster reefs with an inundation duration of > 50%, wave attenuation would increase with width; and (3) there would be a difference in wave transmission between shell-based and concrete-based oyster reefs. Furthermore, at the Virginia and Florida reefs, we compared the wave height attenuation of oyster reef living shorelines to rock sills and natural unrestored oyster reefs, respectively.

Methods

Study locations

The fifteen oyster reef living shoreline (hereafter, "oyster reef")-control pairs (Fig. 1) were selected to cover the diversity of techniques commonly employed, which varied within and among states in terms of age, materials, and size (Table 2; Appendix S1: Table S1). The wave climate in the offshore waters at each location was observed at the NDBC (National Data Buoy Center) stations (Appendix S1: Fig. S1), and the wind field was observed at the closest NOAA (National Oceanic and Atmospheric Administration) climate station (Appendix S1: Fig. S1) over a two-year period from 2017 – 2018 and during the study period at each location (one week). Wind fetch distances were calculated for each site using fetchR (Seers 2018).

New Jersey/Delaware

Study sites at Nantuxent (NJ1; 39.2848, -75.2361) and Gandy's Beach (NJ2; 39.2789, -75.2430) were located on the western shore of New Jersey; the site at Mispillion (NJ3; 38.9477, -

75.3149) was located on the eastern shore of Delaware, in Delaware Bay (Table 2). In 2016, nine shell bag oyster reefs were installed at Gandy's Beach on land owned by The Nature Conservancy, and a series of Oyster Castles® were installed at Nantuxent next to Money Island Marina (The Nature Conservancy 2017). These sites have high value, both economically (Money Island Marina was the off-load point for the NJ commercial oyster fleet) and environmentally (Gandy's Beach is a nesting site for horseshoe crabs and a feeding ground for the migrating red knot). Oyster Castles® were also installed at the mouth of the Mispillion River, immediately adjacent to the DuPont Nature Center (Moody et al. 2016), situated across the river from a large breakwater present on the bay-side. This site is a common feeding area for red knots during their spring/summer migration, is home to one of a few naturally occurring intertidal oyster reefs in Delaware, and the aim was to expand the natural oyster reef to stabilize eroding saltmarsh.

The tides in Delaware Bay are semi-diurnal, and the mean tidal range is 1.7 m (NOAA station 8535055; Table 2). In the offshore waters, the predominant wave direction is from the east and south-east, with an average significant wave height of 1.05 m from this direction in the period 2017 – 2018, and 0.83 m during the study period (Appendix 1: Fig. S2). The predominant wind direction is from the west, where the greatest wind speeds were recorded during the study period (Appendix 1: Fig. S3). This corresponded to the direction with the largest fetch distances at NJ1 and NJ2 (Appendix S1: Table S1). During the deployment at NJ3, wind speeds were low (< 4 ms^{-1}) from the east and south.

Virginia

Diggs (VA3; 37.4473, -76.2605) was located in Chesapeake Bay and Laws (VA1; 36.8973, -76.2721) and Captain Sinclair (VA2; 37.3245, -76.4275) were located in two sub-estuaries of Chesapeake Bay, the Lafayette River and Mobjack Bay, respectively (Table 2). The oyster reefs were constructed in 2016 – 2017 as erosion control for private waterfront properties and were made of Ready Reef, Oyster Castles® and bagged shell for Diggs, Laws, and Captain Sinclair, respectively. At all of the sites, there was also a section of shoreline protected by a rock sill with saltmarsh.

The tides in Chesapeake Bay are semi-diurnal and the mean tidal range is 0.7 m (NOAA station 8637689; Table 2). In the offshore waters, the predominant wave direction is from the east and south-east, with an average significant wave height of 0.93 m from this direction in the period 2017 –

2018, and 0.68 m during the study period (Appendix 1: Fig. S2). A southerly wind was predominant during the study period (Appendix 1: Fig. S3), which corresponded to the direction of the highest fetch at VA1 and VA2 (Appendix S1: Table S1). Although, the strongest wind (above 8 m s^{-1}) was recorded from the north during the study, the direction with the largest fetch at VA3 (Appendix S1: Fig. S3; Table S1).

Florida

Florida sites were located on the east coast of Central Florida in Mosquito Lagoon, which encompasses the northernmost section of the Indian River Lagoon system (Table 2). The tides are semi-diurnal and the mean tidal range is 0.3 m (NOAA station 8721222; Table 2). The Indian River Lagoon System is long (195 km), shallow (1-3 m) and narrow (2-4 km), making it extremely fetch-limited (Appendix S1: Table S1) and only persistent south-east or north-west winds tend to cause flooding and erosion (Colvin et al. 2018). During the study the predominant winds were from the south and southwest (Appendix 1: Fig. S3). In the offshore waters, the predominant wave direction is from the east and northeast, with an average significant wave height of 1.18 m from this direction in the period 2017 – 2018, and 0.48 m during the study period (Appendix 1: Fig. S2).

The oyster reefs Mosquito (FL1; 25.9589, -80.8746), Hallmark (FL2; 28.9684, -80.8803) and Pufferfish (FL3; 28.9699, -80.8818) were oyster reef restoration projects constructed in 2010, 2017 and 2016, respectively using the oyster mat method (oyster shells attached to aquaculture grade mesh; www.restoreourshores.org). The oyster reefs were restored on the historic footprint of degraded natural reefs, and at all sites there were natural unrestored oyster reefs adjacent to the oyster reef living shoreline.

Alabama

Alabama study sites were located in Portersville Bay; Northeastern Point aux Pines (AL1; 30.3881, -88.2943) was on the north-eastern portion of a peninsula in the bay (Sharma et al. 2016), while Coffee Island 1 and 2 (AL2, AL3; 30.3428, -88.2552) were on the eastern shoreline of Coffee Island (or Isle aux Herbes) (Table 2). The Point aux Pines reef was constructed in 2009 comprising three 25 m units of loose shell. The Coffee Island reefs, constructed in 2010, were made of experimental units of bagged shell, ReefBLK^{SM} and Reef Ball^{TM}, the latter two were used in this study (Heck et al. 2012).

The tides in Portersville Bay are diurnal and the mean tidal range is 0.4 m (NOAA station 8735180; Table 2). In the offshore waters, the predominant wave direction is from the south and south-east, with an average significant wave height of 0.89 m from this direction in the period 2017 – 2018, and 0.57 m during the study period (Appendix 1: Fig. S2). The most persistent winds during the study were from the east and south-east (Appendix 1: Fig. S3), which also corresponded to the direction of greatest fetch at these sites (i.e., south and east; Appendix S1: Table S1). The small percentage of wind events > 10 m s^{-1} from the south/east direction were not captured in this study, which likely result in the greatest wave events at these sites.

Louisiana

The sites were in the Biloxi Marsh estuary in Eloi Bay (LA1, LA2; 29.7760, -89.4071) and Lake Athanasio (LA3; 29.7459, -88.4688) in southeastern Louisiana (Table 2). This location has diurnal tides with a mean tidal range of 0.4 m (NOAA station 8761305; Table 2). In Eloi Bay, the living shoreline was constructed by the Coastal Protection and Restoration Authority of Louisiana (CPRA) in 2016 to reduce wave energy in order to minimize adjacent marsh erosion and provide a platform for oysters to grow on. A coastal engineering analysis based on wave attenuation and stability was used to determine the final living shoreline design, which incorporated multiple bioengineered designs, including Wave Attenuation Devices (WAD®) and ShoreJAX^{TM}, which were used in this study (Carter et al. 2016). At Lake Athanasio an Oysterbreak^{TM} shoreline protection reef was built by The Nature Conservancy in 2011. Wave data for the period 2017 – 2018 were not available for these sites, however, modelling by CHE (2014) showed that the annual average wave height at the CPRA reefs between 1980 - 2012 was 0.43 m (Appendix 1: Fig. S2). Relatively low wind speeds (< 6 ms^{-1}) were recorded predominantly from the northwest and west during the study. The largest fetch distances are from the south and east at the sites in this location, which was the prevailing wind direction during 2017 – 2018 (Appendix S1: Table S1, Fig. S2).

Data collection

Wave loggers (RBR®*solo* D wave; hereafter RBRs) were deployed for 48 hours (36 hrs for NJ2, NJ3 and FL2 due to tide times and distance to travel between sites) at each reef, rotated over 5 weeks in June - July 2018. At each site four RBRs were deployed at a control (no reef) and oyster reef treatment; one each placed offshore and onshore of the control or reef area (~ 2-5 m from the on- and off- shore reef edge; Fig. 1). The control was selected to be as close to the reef as possible (site dependent; a minimum of ~ 10 m), yet outside the reef zone of wave influence, maintaining similar shoreline characteristics (e.g. vegetation, substrate type), orientation and fetch. The RBRs were attached with cable ties to a metal or PVC pole that was hammered into the seabed and the transect length between the onshore and offshore RBRs at each treatment was measured. The RBRs were programmed using the software Ruskin (v1.13.12; mode = wave; frequency = 1 Hz; duration = 1024; burst rate = 1 hour) to collect wave data (significant wave height, H_s, in metres and associated period, T, in seconds). The wave data collected is assumed to be primarily wind-driven, however, boat wakes may also be important wave sources in some locations (Garvis 2009) and could have contributed to the wave heights in this study.

At LA1 and LA2, five RBRs were deployed: two placed onshore and offshore of the control and three placed around two replicate reefs (two onshore of each reef and one offshore of the reefs). A different set-up was used due to the difficulty of returning to the sites over multiple days to rotate the RBRs (5 RBRs were the maximum we had available). As the reefs were aligned with a similar orientation along the shoreline, we assumed that the offshore wave energy would be consistent between reefs. There was no significant difference between the wave heights recorded at the offshore RBR for the control and reef treatments ($t_{(37)} = -1.1996$, $P > 0.05$), providing further support of this assumption.

Ten photo-quadrats ($0.09\ m^2$) were taken of each reef at New Jersey, Delaware, Virginia and Florida and the percentage cover of oysters was calculated using 25 random points assigned using the program CPCe4.1 (Kohler and Gill, 2006). The percentage cover of oysters could not be quantified at Alabama or Louisiana as water levels were too high during the sampling period and the water too turbid to take photo-quadrats. The size of the reef (length, width, height) and distance from shoreline was either measured in the field during RBR deployment or determined from aerial imagery using ArcGIS. All reefs were positioned parallel to the shore.

In Virginia and Florida, rock sills and natural oyster reefs were added as an additional treatment to the experimental design, respectively. In Virginia, rock sills were present at all sites adjacent to the oyster reef living shoreline, and two additional RBRs were positioned onshore and offshore of the structure at the same time as the oyster reef and control treatments, as before. Unfortunately, one RBR was lost in a storm during the last deployment in Virginia, which left five for deployment in Florida. Therefore, in Florida one RBR was placed onshore of the natural oyster reefs, and the offshore wave height was assumed to be the same as that for the oyster reef living shoreline, as before. At all sites, the natural oyster reef was directly in line and adjacent to the oyster reef living shoreline. There was, however, a significant difference in the wave heights recorded between the offshore RBR for the control and oyster reef living shoreline treatments ($t_{(122)} = -3.9571$, $P < 0.001$), although the mean ± SE was similar for both treatments (0.01 ± 0.001 m).

Wave analysis

The absolute pressure values recorded by the RBRs were converted to gauge pressure using atmospheric pressure data obtained from the closest weather stations to each site (Appendix S1: Fig. S1; Morris et al. 2019b). Wave data were post-processed to account for shoaling and breaking, where appropriate, using the method detailed in Haynes (2018) and (Morris et al. 2019b). Water densities were calculated using the Thermodynamic Equation of Seawater – 2010 (TEOS-10; IOC et al. 2010), using the known salinity at each location and water temperatures obtained from World Sea Temperatures (www.seatemperature.org). The corrected pressure data were then converted to water depth using this calculated water density (Eq. 1),

$$d = \frac{P}{\rho_w g} \qquad \text{(Eq. 1)}$$

where d is the water depth, P is the pressure, ρ_w is the density of water, and g is the acceleration due to gravity.

The water levels were linearly detrended to remove low-frequency signal, which provided an average water depth for each burst (of 1024 samples per hour, as above) and a zero-average input for

Fast-Fourier-Transform. A pressure response factor, K_p, was determined for each frequency bin of the Fast-Fourier-Transform (Eq. 2; Kamphuis 2010),

$$K_p = \frac{\cosh(k(d+z))}{\cosh(kd)} \qquad \text{(Eq. 2)}$$

where k is the wave number, d is the water depth, and z is the logger level from the surface. The wave energy density spectrum was then corrected for depth by dividing it by the pressure response factor squared. The output wave energy density spectrum was divided into sea (1 to 10 s period) and swell (10 to 20 s period) components (USACE 1984). Significant wave heights for each logger (H_s; using the zeroth-moment wave height) were determined from the wave spectrum (Eq. 3; Moeller et al. 1996),

$$H_s = 4\sqrt{\frac{E_{total}}{(\rho_w g)}} \qquad \text{(Eq. 3)}$$

where E_{total} is the total energy defined as the integral of the wave energy density spectrum. The wave period corresponding to the significant wave height, $T_{1/3}$, was approximated as $1.2\,T_{m01}$, where T_{m01} is the zero-crossing period (Eq. 4; Goda 2010),

$$T_{m01} = \sqrt{\frac{m_0}{m_2}} \qquad \text{(Eq. 4)}$$

where m_0 and m_2 are the zeroth and second moments of the wave energy density spectrum, respectively. Linear wave theory was used to calculate wave length, celerity and group velocity, based on wave conditions at the offshore logger and assuming wave period did not change as the wave approached shore. Wave celerity at the onshore RBR within each treatment at a site was estimated based on Hunt (1979). This was used to calculate the shoaling coefficient (Eq. 5; Haynes 2018),

$$K_s = \sqrt{\frac{C_{g\_off}}{C_{g\_on}}} \qquad \text{(Eq. 5)}$$

where C_{g_off} is the offshore RBR wave group celerity, and C_{g_on} is the onshore RBR wave group celerity. Predicted onshore wave heights were generated to account for shoaling (Eq. 6) and breaking (using the co-efficient of 0.78 multiplied by the depth at the onshore gauge; Haynes 2018),

$$H_{s\_pred} = H_{s\_off} K_s \qquad \text{(Eq. 6)}$$

where H_{s_pred} is the predicted wave height and H_{s_off} is the offshore wave height. The wave transmission coefficient was defined as the ratio of measured to predicted wave height (Eq. 7; Haynes 2018), where the predicted wave height was the limiting of the shoaling or breaking wave height,

$$K_t = \frac{H_{s\_on}}{H_{s\_pred}} \qquad \text{(Eq. 7)}$$

where H_{s_on} is the recorded wave height at the onshore RBR. The wave transmission coefficient accounts for potential changes in wave height due to shoaling and breaking, but not other processes that could not be controlled for in this study (e.g., refraction and diffraction). All processing was done in MATLAB (MathWorks 1996) and resulted in hourly data for water depth, significant wave height at each RBR, wave period and the wave transmission coefficient during the period the RBRs were underwater (i.e. only at high tide for most locations).

The freeboard (m) was calculated as the reef height minus the water depth. The inundation duration was calculated as the percentage of time the entire reef was submerged (i.e., the freeboard had a negative value) during the study period. The inundation period during the study was compared to longer-term data using water levels at nearby USGS gauges (NOAA tides and currents for Alabama; Appendix S1: Fig. S1). The difference between the reef crest elevation and water level relative to NAVD88 was used to calculate the percentage of time the crest of the reef was inundated. The reefs were categorised into more or less than 50% inundated; this threshold was chosen as the lower limit of inundation for *C. virginica* (Table 1). Regression slopes between onshore measured and predicted significant wave heights were compared for controls, and oyster reefs based on inundation duration, width and construction material. Further the wave heights were compared at controls, oyster reefs and either rock sills or natural oyster reefs, at Virginia and Florida respectively. The effect of location (fixed, 3 levels: New Jersey, Virginia, Florida), inundation duration (fixed, percentage), and age (fixed, years) on the percentage cover of oysters was tested using a linear mixed effects model, with site nested in location included as a random factor on log transformed data. A likelihood ratio test comparing the model with and without site was used to obtain a p-value for this random effect. All analyses were done in R 3.4.0 (R Core Team 2017).

Results

Significant wave heights recorded at the sites ranged from 0 – 0.35 m during the study period (Fig. 2a). Average water depth between the gauge pairs ranged from 0.16 – 2.35 m (Fig. 2b), after reef emersion time was truncated from each data set (i.e., low tide). The NJ2 site experienced the greatest depth of inundation (freeboard = -1.88 m) due to a combination of the low height of this reef and New

Jersey experiencing the greatest tidal range (Table 2), with a potential contribution of the greater wave heights recorded during the study period (Fig. 2a). The LA1 and LA2 sites experienced the least inundation (freeboard = 0.86 m), with the crests exposed 100% of the time (Table 2). The average freeboard of all reefs is listed in Appendix 1: Table S1.

Three out of the 15 reefs had an inundation duration of less than 50% (FL1, LA1, LA2), while the other 12 reefs were inundated more than 50% of the time and considered to be within the tolerable aerial exposure limits for *C. virginica* (Table 1). Two reefs were fully inundated during the study (AL1, AL2; Table 1, Fig. 2b). The categorisation of the reefs based on the measured study conditions aligned with that estimated from the USGS gauges during the study and longer-term from 2017-2019 (Table 1). In general, the inundation durations measured during the study were representative of the longer-term data (Table 1), but at VA3 the inundation duration was 30-40% greater during the study compared to the long-term data (Table 1). This is likely due to the storm event captured causing wind and/or wave set-up, which generated the second highest wave heights in the study (after NJ2; Fig. 2a). Similarly, the inundation duration at FL3 was 20% less, and at AL3, 40% more during the study compared to the long-term data. The reason for these differences is less clear but is likely due to the water level data from the USGS gauges not being site specific, and therefore providing an estimation only.

There was little difference between the percent change in wave height between the controls (5.9%) and oyster reefs that experienced greater than 50% inundation duration (4.5%; Fig. 3a, b). In contrast, a 68.4% decrease in wave height was observed at reefs that were inundated for less than 50% of the time (Fig. 3b). Despite this, when the freeboard was the same between reefs that had either greater or less than 50% inundation duration, the wave attenuation was also similar (Fig. 4). Wave transmission significantly decreased with increasing positive freeboard and decreasing submergence for both inundation regimes (Fig. 4). Thus, the overall result of a lower wave attenuation of reefs that have a greater inundation duration is driven by these reefs experiencing less time at the optimal freeboard for wave attenuation (i.e., a reef crest elevation that is either at or above the water level). Reefs that had an inundation duration of greater than 50% were categorised based on the range of widths to determine if reefs of a greater width had a lower wave transmission. Based on the range of reef widths observed in this study, width had little effect on the wave transmission of these reefs (Fig.

3c). Whether the reefs were made of shell or concrete also had less of an effect on wave transmission compared to reef height (Fig. 3d).

On average, the rock sills were 2.5 times taller than the oyster reefs in Virginia and spent 35% or less time inundated during the study (Table 2). Rock sills reduced wave heights by 72% compared to a 5% and 3% reduction in wave height at oyster reefs and controls, respectively (Fig. 5a). In Florida, the restored oyster reefs were a similar width and height as the natural unrestored reefs, with the latter having a slightly taller profile at FL2 and FL3 (Table 2). The wave attenuation was greatest at the natural reefs (84%), followed closely by the restored oyster reefs (75%), compared to the controls (35%; Fig. 5b). However, the percent of variance explained by the linear model was lower at the natural (15%) and restored (31%) oyster reefs.

There was no significant effect of location ($F_{3,44}$=0.03, P>0.05), inundation duration ($F_{1,4}$=0.23, P>0.05), or age ($F_{1,4}$=0.01, P>0.05) on the percentage cover of oysters. However, there was a significant difference in the oyster cover among sites (P<0.001; Table 1).

Discussion

To achieve the goal of a sustainable coastal defense structure, oyster reef living shorelines must be effective at both hazard risk reduction and habitat provisioning for oysters. Understanding the coastal protection afforded by reefs within the habitat limitations of oysters is therefore important for identifying the parametric ranges for which oyster reefs and coastal defense overlap. Oyster reefs where the crest was inundated less than 50% of the time were almost 14 times more effective at reducing the wave heights observed during this study than those that had an inundation duration of more than 50%. The width of the reefs that had > 50% inundation ranged from 0.6 – 6.6 m; these widths had little effect on the wave transmission of the reefs. Eight out of the nine study sites where oyster colonisation could be quantified experienced the optimal inundation regime. However, the percentage cover of oysters varied among these sites, with no effect of inundation duration, age, or location.

The duration and depth of inundation are determined by the intertidal elevation of the reef and the tidal amplitude of an area (Byers et al. 2015), as well as periodic events such as storm-driven wind or wave set-up. The duration and depth of inundation have an effect on wave attenuation and on oyster recruitment, survival, and growth. Previous research has shown that oyster reefs are very effective at attenuating waves when the reef crest height is at, or above, the water level (Chauvin 2018, MacDonald 2018, Wiberg et al. 2018, Chowdhury et al. 2019, Zhu et al. 2020, Spiering et al. in revision). This is because waves are strongly modified or break as they cross the reef (Wiberg et al. 2018). As the water levels increase, a reduction in wave height is instead caused by the interaction of oscillatory motion with the reef, the effect of which decreases with increasing water depth (Wiberg et al. 2018). Here, our data support this finding, showing that the negative relationship between wave transmission and reef submergence is evident across the large biogeographic scale studied.

It has been noted previously that some of the reefs studied may only spend 10-25% of the time at the optimal freeboard for wave attenuation (MacDonald 2018, Wiberg et al. 2018, Zhu et al. 2020). When reefs become submerged, the wave attenuation can decrease to 0-20% (Wiberg et al. 2018; Fig. 4). However, this inundation duration is within the optimal range for oyster population establishment (Table 1). Critically, *C. virginica* do not tend to colonise substratum where the inundation duration is less than approximately 50% (Ridge et al. 2015; Table 1). Reefs with crests above this threshold will not be colonised by oysters, although if the reef base is within the optimal range then oyster habitat may be provided lower on the structure, but this will not result in an oyster reef that can build and maintain itself (i.e., wave attenuation is provided by the artificial reef base not the growing oyster reef; Morris et al. 2019). Greater submergence times enhance feeding, and therefore growth of oysters (Solomon et al. 2014), and reduce desiccation stress. Too much immersion time, however, can negatively affect oysters due to greater fouling or predation in the subtidal (Fodrie et al. 2014). Thus, there is an optimum inundation duration that varies slightly along the geographical range, but seems to be within a 5-40% range (Table 1). This translates to oyster reefs spending a greater percentage of time outside of the freeboards that maximize wave attenuation, and can explain the overall difference in wave attenuation of reefs that experienced more or less than 50% inundation duration in this study.

The extent to which the inundation duration affects wave attenuation is also dependent on the tidal amplitude. Where the tidal range is low, the variation in wave attenuation will be less than in areas that have a greater tidal range. Although all of the sites here are considered microtidal (defined as a tidal range of 0–2 m as per Davies 1964), they still experienced a range of tidal amplitudes (Table 2), with the reefs in New Jersey having a greater depth of inundation than the other sites. In contrast to its effect on wave attenuation, an increased depth of inundation can have a positive effect on oyster growth and reef height due to a greater volume of water delivery per unit of time and flow velocity that affects feeding and larval delivery (Byers et al. 2015).

For the reefs where the percent cover of oysters could be measured, inundation duration varied between 68-97% for all but one reef (FL1; 38%). This variation was similar to that found across a 1,500 km region from North Carolina to Florida (52-84%; Byers et al. 2015), where there was no effect of inundation duration across latitude, and therefore oyster reef properties. There was, however, significant variation in percent cover of oysters among sites in this study that was not a factor of inundation duration. Other physical variables that commonly affect oyster reef properties are salinity and temperature (Byers et al. 2015). Temperature linearly declines with increasing latitute, but as there was no effect of location on oyster cover, it is unlikely to be the cause of the site variability. Similarly, given that oysters are found in each of the areas studied, the salinity was considered to be suitable. Another factor that affects the recruitment of reef substratum is larval availability. The reefs in this study relied on natural recruitment from the water column. If the reefs are recruitment-limited then they may never establish an oyster population; larval dispersal and connectivity are therefore important considerations in the siting of reef substratum (Lipcius et al. 2008, Puckett et al. 2018). Further, as coastal defenses are inherently built in turbulent, wave exposed environments, an added variable of the threshold of exposure for oyster reef establishment is critical in oyster reef living shorelines (Whitman and Reidenbach, 2012). The benthic flow across the reef can be manipulated to enhance larval recruitment by increasing topographic complexity that creates interstitual spaces, which lower the shear stresses that can dislodge larvae (Whitman and Reidenbach, 2012).

The comparison of rock sills to oyster reefs further supports the importance of crest height for wave attenuation in narrow structures. Rock sills showed a similar magnitude of wave height reduction as the oyster reefs that were exposed for more than 50% of the time, which again was much greater than the oyster reefs in Virginia that all had <50% exposure. When oyster reef living shorelines were compared to natural reefs in Florida, the wave attenuation was similar between the two treatments (75% and 84%, respectively), and double that of the control (35%). This is likely due to the similarity in size (height and width) of the restored and natural reefs, as the restored reefs were deployed onto the historic footprint of natural degraded reefs. However, the natural reefs had a very low percent cover of live oyster compared to the restored reefs (except FL1). Live oysters increase bed roughness and therefore drag, which can lead to better flow energy attenuation (Kitsikoudis et al. 2020). In contrast, degraded reefs consist of loose disarticulated shells that can be moved around with wave events. Therefore, even though the wave attenuation observed was similar between restored and natural degraded reefs here, it is unclear how this may evolve through time, as degraded reefs could eventually disintegrate if not colonised by oysters (Kitsikoudis et al. 2020). The pattern of wave attenuation across treatments in Florida, when considered alone, was very different to the overall patterns observed, as greater attenuation was recorded at both the control and oyster reefs, but it was also more variable. This is likely due to Florida experiencing only very small wave heights for the duration of the deployment. Smaller, high frequency waves (e.g., 1 s period) may have been under-sampled with the 1 Hz frequency used to compare treatments in this study, which potentially resulted in the reporting of smaller wave heights than were present. However, similar maximum wave heights have been recorded at other sites in Mosquito Lagoon, Florida, using a 32 Hz sampling frequency (Kibler et al. 2019), thus our results are just as likely to be due to the calm weather during deployments and the fact that these sites are very sheltered under normal conditions.

At the other locations, there was a range in wave heights observed and these were comparable to those in previous studies in New Jersey (average 0.03 - 0.11 m, maximum 0.15 - 0.55 m; MacDonald 2018), Virginia (average 0.03 - 0.10 m, maximum 0.30 - 0.50 m; Wiberg et al. 2018) and Louisiana (average 0.10 m, maximum 0.45 m; Chauvin 2018). Nevertheless, these wave heights were generally more representative of calm to average conditions due to the trade-off between the large-scale of the study and wave sensor deployment duration (36 - 48 hours), which limited the range of wave conditions that could be observed. The size of the waves (Wiberg et al. 2018, Chowdhury et al. 2019), as well as whether they are swell- or wind-dominated (Zhu et al. 2020) or accompanied by storm tides, impacts the efficacy of oyster reefs at wave attenuation. Previous studies of oyster reefs have shown that for the equivalent water depth, wave attenuation increases with wave height (Wiberg et al. 2018, Chowdhury et al. 2019). This may explain why fringing oyster reefs have been found to have a greater impact on shoreline retreat at higher exposure locations (La Peyre et al. 2015). Hence, there is the potential that with larger wave heights the wave transmission values observed in this study could decrease at oyster reef living shorelines. This highlights the need to examine multiple reefs experiencing diverse conditions to get a complete understanding of how they work.

It is also important to consider the type of shoreline being protected, as habitat type can influence susceptibility to erosion from different weather events. For example, saltmarsh was the predominant shoreline type in our study. Leonardi et al. (2016) demonstrated that marsh-edge erosion was caused by moderate, but high frequency (2.5 ± 0.5 per month) storms. Larger storms, in contrast, are often accompanied by storm surge, which dissipates over the marsh bed rather than impacting the marsh edge. Previous research on oyster reef living shorelines has shown significant variability in erosion control of saltmarsh among sites (Meyer et al. 1997, Piazza et al. 2005, Stricklin et al. 2010, Scyphers et al. 2011, La Peyre et al. 2013, Moody et al. 2013, La Peyre et al. 2014, 2015). Oyster reefs are likely to have the greatest effect on the reduction of saltmarsh erosion when the elevation of the marsh platform coincides with the water depths that maximize wave attenuation (i.e., when reef submergence is low; Wiberg et al. 2018). As currently designed, reefs that are within the habitat requirements for oysters are likely to have little effect on higher-elevation shorelines dominated by saltmarshes. How this process translates to protection by oyster reefs for other shoreline habitat types is not well known.

Natural oyster reefs were once vast, with historical imagery suggesting reefs kilometres long fringed the shorelines in the 1800s in Chesapeake Bay, Virginia (Woods et al. 2005). A recent study in Mosquito Lagoon, Florida, found that small-scale restored oyster reefs (as studied here) had a cumulative positive impact on erosion rates that may not be observed at a single site (McClenachan et al. 2020). The variability in effectiveness of oyster reefs at providing erosion control may be the result of a mismatch in the scale of the construction of living shorelines and that required for delivery of the coastal defense service. For example, McClenachan et al. (2020) demonstrated that the combined 89 smaller oyster reef projects had a landscape scale effect within this ecosystem. At an individual scale, the reefs we studied were narrow structures. The range of widths observed had little effect on the wave attenuation of the reefs that were at the appropriate elevation for oysters. However, physical modelling of submerged rubble-mound breakwaters (Seabrook and Hall, 1998) and bagged oyster shell reefs (Allen and Webb, 2011) showed that wider structures of the same elevation can further decrease wave transmission by 20-40%. Field studies have shown width to be important for wave attenuation in saltmarshes (Shepard et al. 2011) and coral reefs (Ferrario et al. 2014), however, this factor has not been examined for oyster reefs. This is likely due to most of our knowledge on the wave transmission of oyster reefs being generated from studies on living shorelines, with a paucity of information available on natural reefs (Narayan et al. 2016). For living shorelines to be used as a tool for restoration and risk reduction, it is imperative that we optimize the design to maximize both ecological and engineering outcomes.

Conclusions

In the face of a changing climate, there is an increasing interest in living shorelines as an adaptive and sustainable coastal defense strategy. For living shorelines to be successful, they need to establish a self-sustaining population of the target species and have the ability to provide coastal protection under the conditions that cause erosion and/or flooding. This large-scale study across multiple states provides a broader perspective on the diversity of oyster reef living shoreline approaches. We showed that many of the living shoreline approaches using oysters failed to optimize the ecological and engineering goals. To date, studies have focused on understanding the wave attenuation of oyster reefs without integrating consideration for the ecological limitations of oysters. This has resulted in a focus on how the crest of the reef influences wave transmission. However, given that this design parameter needs to stay within the optimal inundation duration for oysters, efforts should be refocused to understand the effects of other design parameters, such as reef width, on maximising wave attenuation over a greater inundation range. This approach should apply generally to the design and implementation of living shorelines, where the engineering parameters are calculated to account for the ecological limitations of a species in order to achieve both goals. Identifying the circumstances under which living shorelines can be designed to achieve these goals is also important to determine the thresholds for their use successfully. Our results suggest that the low-crested, narrow oyster reefs that are commonly built are, on average, not effective at wave attenuation. Their ability to provide erosion control, however, will also depend on the elevation of the shoreline and the conditions that contribute to local erosion. This combination of factors has likely contributed to the large variation in erosion control by oyster reef living shorelines reported in the literature. A broader understanding of the reef characteristics and seascape contexts that result in effective coastal defense by oyster reefs is needed to inform the design of future living shoreline projects. This continued research effort will ensure that oyster reef living shorelines are successful in achieving both their ecological and engineering goals.

Acknowledgments

We thank T. Graham for his advice on data processing and J. Shinn for her assistance with the New Jersey sites. R.L.M. was supported by an Early Career Researcher Global Mobility Grant from The University of Melbourne. The National Centre for Coasts and Climate is funded through the Earth Systems and Climate Change Hub by the Australian Government's National Environmental Science Program. This paper is Contribution No. 3990 of the Virginia Institute of Marine Science, William & Mary. Any use of trade, firm, or product names is for descriptive purposes only and does not imply endorsement by the U.S. Government. Author Contributions: RLM conceived the idea and all authors contributed to the experimental design. RLM led the data collection with help from all authors; RLM conducted the analysis. All authors contributed critically to the data interpretation and drafts, and gave final approval for publication. The authors have no conflicts of interest to declare.

Supporting Information

Additional supporting information may be found online at: [link to be added in production]

Open Research

Data (Morris et al. 2021) are available on FigShare from The University of Melbourne at" https://doi.org/10.26188/13833089

References

Allen, R. J., and B. M. Webb. 2011. Determination of wave transmission coefficients for oyster shell bag breakwaters. Coastal Engineering Practice:684-697.

Beck, M. W., R. D. Brumbaugh, L. Airoldi, A. Carranza, L. D. Coen, C. Crawford, O. Defeo, G. J. Edgar, B. Hancock, M. C. Kay, H. S. Lenihan, M. W. Luckenbach, C. L. Toropova, G. F.

Zhang, and X. M. Guo. 2011. Oyster reefs at risk and recommendations for conservation, restoration, and management. Bioscience 61:107-116.

Bilkovic, D. M., M. Mitchell, P. Mason, and K. Duhring. 2016. The role of living shorelines as estuarine habitat conservation strategies. Coastal Management 44:161-174.

Bulleri, F., and M. G. Chapman. 2010. The introduction of coastal infrastructure as a driver of change in marine environments. Journal of Applied Ecology 47:26-35.

Byers, J. E., J. H. Grabowski, M. F. Piehler, A. R. Hughes, H. W. Weiskel, J. C. Malek, and D. L. Kimbro. 2015. Geographic variation in intertidal oyster reef properties and the influence of tidal prism. Limnology and Oceanography 60:1051-1063.

Carter, J., C. Connor, J. Todd, A. Agarwal, and H. Bermudez. 2016. Living shoreline demonstration project, prepared for Louisiana Coastal Protection and Restoration Authority. Coast and Harbor Engineering, a division of Mott MacDonald, New Orleans.

Casas, S. M., J. La Peyre, and M. K. La Peyre. 2015. Restoration of oyster reefs in an estuarine lake: population dynamics and shell accretion. Marine Ecology Progress Series 524:171-184.

Chauvin, J. M. 2018. Wave attenuation by constructed oyster reef breakwaters. Louisiana State University, Louisiana, US.

Chowdhury, M. S. N., B. Walles, S. M. Sharifuzzaman, M. Shahadat Hossain, T. Ysebaert, and A. C. Smaal. 2019. Oyster breakwater reefs promote adjacent mudflat stability and salt marsh growth in a monsoon dominated subtropical coast. Scientific Reports 9:8549.

Coast and Harbor Engineering, CHE. 2014. Living Shoreline Demonstration Project, Coastal Engineering and Alternatives Analysis. Baton Rouge, LA. October 9, 2014.

Coen, L. D., and A. T. Humphries. 2017. Chapter 19. Oyster-generated marine habitats: their services, enhancement and monitoring. In: S. Stuart and S. Murphy (eds) Routledge Handbook of Ecological and Environmental Restoration, Routledge: New York, 274-294.Colvin, J., S. Lazarus, M. Splitt, R. Weaver, and P. Taeb. 2018. Wind driven setup in east central Florida's Indian River Lagoon: forcings and parameterizations. Estuarine, Coastal and Shelf Science 213:40-48.

Coghlan, I. R., Howe, D. and W. C. Glamore. 2016. Preliminary testing of oyster shell filled bags. WRL Technical Report 2015/20, January.

Davies, J. L. 1964. A morphogenic approach to world shorelines. Zeitschrift Fur Geomorphologie 8:27-42.

Ferrario, F., M. W. Beck, C. D. Storlazzi, F. Micheli, C. C. Shepard, and L. Airoldi. 2014. The effectiveness of coral reefs for coastal hazard risk reduction and adaptation. Nature Communications 5:3794.

Fodrie, F. J., A. B. Rodriguez, C. J. Baillie, M. C. Brodeur, S. E. Coleman, R. K. Gittman, D. A. Keller, M. D. Kenworthy, A. K. Poray, J. T. Ridge, E. J. Theuerkauf, and N. L. Lindquist. 2014. Classic paradigms in a novel environment: inserting food web and productivity lessons from rocky shores and saltmarshes into biogenic reef restoration. Journal of Applied Ecology 51:1314-1325.

Garvis, S. K. 2009. Quantifying the impacts of oyster reef restoration on oyster coverage, wave dissipation and seagrass recruitment in Mosquito Lagoon, Florida. University of Central Florida, Florida, United States.

Goda, Y. 2010. Random seas and design of maritime structures. World Scientific Publishing Co. Pte. Ltd., Singapore.

Grabowski, J. H., R. D. Brumbaugh, R. F. Conrad, A. G. Keeler, J. J. Opaluch, C. H. Peterson, M. F. Piehler, S. P. Powers, and A. R. Smyth. 2012. Economic valuation of ecosystem services provided by oyster reefs. Bioscience 62:900-909.

Haynes, K. M. 2018. Field measurements of boat wake attenuation in coastal salt marshes. University of South Alabama.

Heck, K., J. Cebrian, S. Powers, R. Gericke, C. Pabody, and J. Goff. 2012. Final Monitoring Report to the Nature Conservancy: Coastal Alabama Economic Recovery and Ecological Restoration Project: Creating jobs to protect shorelines, restore oyster reefs and enhance fisheries productions, Dauphin Island Sea Lab and University of South Alabama, Dauphin Island.

Hernandez, A. B., R. D. Brumbaugh, P. Frederick, R. Grizzle, M. W. Luckenbach, C. H. Peterson, and C. Angelini. 2018. Restoring the eastern oyster: how much progress has been made in 53 years? Frontiers in Ecology and the Environment 16:1-9.

Hinkel, J., D. Lincke, A. T. Vafeidis, M. Perrette, R. J. Nicholls, R. S. J. Tol, B. Marzeion, X. Fettweis, C. Ionescu, and A. Levermann. 2014. Coastal flood damage and adaptation costs under 21st century sea-level rise. Proceedings of the National Academy of Sciences 111:3292-3297.

Hunt, J. N. 1979. Direct solution of wave dispersion equation. Journal of Waterway, Port, Coastal, and Ocean Engineering 4:457-459.

IOC, SCOR, and IAPSO. 2010. The international thermodynamic equation of seawater – 2010: calculation and use of thermodynamic properties. Intergovernmental Oceanographic Commission, Manuals and Guides No. 56, UNESCO.

Kamphuis, J. W. 2010. Introduction to coastal engineering and management, Advanced series on ocean engineering. World Scientific, Singapore.

Kibler, K. M., V. Kitsikoudis, M. Donnelly, D. W. Spiering, and L. Walters. 2019. Flow–vegetation interaction in a living shoreline restoration and potential effect to mangrove recruitment. Sustainability 11:3215.

Kitskoudis, V., K. M. Kibler, and L. J. Walters. 2020. In-situ measurements of turbulent flow over intertidal natural and degraded oyster reefs in an estuarine lagoon. Ecological Engineering 143:1056882.

Kohler, K. E., and S. M. Gill. 2006. Coral Point Count with Excel extensions (CPCe): A Visual Basic program for the determination of coral and substrate coverage using random point count methodology. Computers and Geosciences 32:1259-1269.

La Peyre, M. K., A. T. Humphries, S. M. Casas, and J. F. La Peyre. 2014. Temporal variation in development of ecosystem services from oyster reef restoration. Ecological Engineering 63:34-44.

La Peyre, M. K., L. Schwarting, and S. Miller. 2013. Preliminary assessment of bioengineered fringing shoreline reefs in Grand Isle and Breton Sound, Louisiana. Report 2013-1040, Reston, VA.

La Peyre, M. K., K. Serra, T. A. Joyner, and A. Humphries. 2015. Assessing shoreline exposure and oyster habitat suitability maximizes potential success for sustainable shoreline protection using restored oyster reefs. PeerJ, 3, e1317.

Leonardi, N., N. K. Ganju, and S. Fagherazzi. 2016. A linear relationship between wave power and erosion determines salt-marsh resilience to violent storms and hurricanes. Proceedings of the National Academy of Sciences 113:64-68.

Lipcius, R. N., D. B. Eggleston, S. J. Schreiber, R. D. Seitz, J. Shen, M. Sisson, W. T. Stockhausen, and H. V. Wang. 2008. Importance of metapopulation connectivity to restocking and restoration of marine species. Reviews in Fisheries Science 16:101-110.

Livingston, R. J., R. L. Howell, X. F. Niu, F. G. Lewis, and G. C. Woodsum. 1999. Recovery of oyster reefs (Crassostrea virginica) in a gulf estuary following disturbance by two hurricanes. Bulletin of Marine Science 64:465-483.

MacDonald, M. 2018. Wave monitoring and sedimentation analysis at four oyster castle breakwaters at Gandy's Beach, NJ. For: The Nature Conservancy. New Jersey, US.

Manis, J. E., S. K. Garvis, S. M. Jachec, and L. J. Walters. 2015. Wave attenuation experiments over living shorelines over time: a wave tank study to assess recreational boating pressures. Journal of Coastal Conservation 19:1-11.

Marshall, D. A. and La Peyre, M. K. 2020. Effects of inundation duration on southeastern Louisiana oyster reefs. Experimental Results 1: E30. doi:10.1017/exp.2020.35.

MathWorks, I. 1996. MATLAB : the language of technical computing : computation, visualization, programming : installation guide for UNIX version 5. Natwick: Math Works Inc., 1996.

McClenachan, G. M., M. J. Donnelly, M. N. Schaffer, P. E. Sacks, and L. J. Walters. 2020. Does size matter?: Quantifying the cumulative impact of small-scale living shoreline and oyster reef restoration projects on shoreline erosion. Restoration Ecology 28:1365-1371.

Meucci, A., I. R. Young, M. Hemer, E. Kirezci, and R. Ranasinghe. 2020. Projected 21st century changes in extreme wind-wave events. Science Advances 6:eaaz7295.

Meyer, D. L., E. C. Townsend, and G. W. Thayer. 1997. Stabilization and erosion control value of oyster cultch for intertidal marsh. Restoration Ecology 5:93-99.

Mitchell, M., and D. M. Bilkovic. 2019. Embracing dynamic design for climate-resilient living shorelines. Journal of Applied Ecology 56:1099-1105.

Moeller, I., T. Spencert, and J. R. French. 1996. Wind wave attenuation over saltmarsh surfaces: preliminary results from Norfolk, England. Journal of Coastal Research 12:1009-1016.

Moody, J., D. Kreeger, S. Bouboulis, S. Roberts, and A. Padeletti. 2016. Design, implementation, and evaluation of three living shoreline treatments at the DuPont Nature Center, Mispillion River, Milford, DE., Partnership for the Delaware Estuary, Wilmington.

Moody, R. M., J. Cebrian, S. M. Kerner, K. L. Heck, S. P. Powers, and C. Ferraro. 2013. Effects of shoreline erosion on salt-marsh floral zonation. Marine Ecology Progress Series 488:145-155.

Morris, R. L., D. M. Bilkovic, M. K. Boswell, D. Bushek, J. Cebrian, J. Goff, K. M. Kibler, M. K. La Peyre, G. McClenachan, J. Moody, P. Sacks, J. P. Shinn, E. L. Sparks, N. A. Temple, L. J. Walters, B. M. Webb, and S. E. Swearer. 2019a. The application of oyster reefs in shoreline protection: are we over-engineering for an ecosystem engineer? Journal of Applied Ecology 56:1703-1711.

Morris, R. L., A. Boxshall, and S. E. Swearer. 2020. Climate-resilient coasts require diverse defence solutions. Nature Climate Change 10:485-487.

Morris, R. L., T. D. J. Graham, J. Kelvin, M. Ghisalberti, and S. E. Swearer. 2019b. Kelp beds as coastal protection: wave attenuation of Ecklonia radiata in a shallow coastal bay. Annals of Botany 125:235-246.

Morris, R., et al. 2021. Morris et al. Ecological Applications.xlsx. University of Melbourne, data set. https://doi.org/10.26188/13833089.v1

Narayan, S., M. W. Beck, B. G. Reguero, I. J. Losada, B. van Wesenbeeck, N. Pontee, J. N. Sanchirico, J. C. Ingram, G. M. Lange, and K. A. Burks-Copes. 2016. The effectiveness. costs and coastal protection benefits of natural and nature-based defences. PLoS ONE 11: e0154735.

Neumann, B., A. T. Vafeidis, J. Zimmermann, and R. J. Nicholls. 2015. Future coastal population growth and exposure to sea-level rise and coastal flooding - A global assessment. PLoS ONE 10:e0118571.

Piazza, B. P., P. D. Banks, and M. K. La Peyre. 2005. The potential for created oyster shell reefs as a sustainable shoreline protection strategy in Louisiana. Restoration Ecology 13:499-506.

Puckett, B. J., S. J. Theuerkauf, D. B. Eggleston, R. Guajardo, C. Hardy, J. Gao, and R. A. Luettich. 2018. Integrating larval dispersal, permitting, and logistical factors within a validated habitat suitability index for oyster restoration. Frontiers in Marine Science 5:75.

R Core Team. 2017. R: A language and environment for statistical computing. R Foundation for Statistical Computing, Vienna Austria. Available online at : http://www.R-project.org

Ridge, J. T., A. B. Rodriguez, F. J. Fodrie, N. L. Lindquist, M. C. Brodeur, S. E. Coleman, J. H. Grabowski, and E. J. Theuerkauf. 2015. Maximizing oyster-reef growth supports green infrastructure with accelerating sea-level rise. Scientific Reports 5:14785.

Ridge, J. T., A. B. Rodriguez, and F. J. Fodrie. 2017. Salt Marsh and Fringing Oyster Reef Transgression in a Shallow Temperate Estuary: Implications for Restoration, Conservation and Blue Carbon. Estuaries and Coasts 40:1013-1027.

Rodriguez, A. B., F. J. Fodrie, J. T. Ridge, N. L. Lindquist, E. J. Theuerkauf, S. E. Coleman, J. H. Grabowski, M. C. Brodeur, R. K. Gittman, D. A. Keller, and M. D. Kenworthy. 2014. Oyster reefs can outpace sea-level rise. Nature Climate Change 4:493-497.

Salvador de Paiva, J. N., B. Walles, T. Ysebaert, and T. J. Bouma. 2018. Understanding the conditionality of ecosystem services: the effect of tidal flat morphology and oyster reef characteristics on sediment stabilization by oyster reefs. Ecological Engineering 112:89-95.

Scyphers, S. B., S. P. Powers, K. L. Heck, and D. Byron. 2011. Oyster reefs as natural breakwaters mitigate shoreline loss and facilitate fisheries. PLoS ONE 6:e22396.

Seabrook, S. and K. Hall. 1998. Wave transmission at submerged rubblemound breakwaters. Coastal Engineering Proceedings 1 (26).

Seers, B. 2018. fetchR: calculate wind fetch.

Sharma, S., J. Goff, R. M. Moody, A. McDonald, D. Byron, K. L. Heck, Jr., S. P. Powers, C. Ferraro, and J. Cebrian. 2016. Effects of shoreline dynamics on saltmarsh vegetation. PLoS ONE 11:e0159814.

Shepard, C. C., C. M. Crain, and M. W. Beck. 2011. The protective role of coastal marshes: a systematic review and meta-analysis. PLoS ONE 6:e27374.

Solomon, J. A., M. J. Donnelly, and L. J. Walterst. 2014. Effects of sea level rise on the intertidal oyster Crassostrea Virginica by field experiments. Journal of Coastal Research 68:57-64.

Spiering, D. W., K. M. Kibler, V. Kitskoudis, M. Donnelly, and L. J. Walters. in revision. Detecting hydrodynamic changes after living shoreline restoration and through an extreme event using a Before-After-Control-Impact experiment. Estuaries and Coasts.

Stricklin, A. G., M. S. Peterson, J. D. Lopez, C. A. May, and C. F. Mohrman. 2010. Do small, patchy, constructed intertidal oyster reefs reduce salt marsh erosion as well as natural reefs? Gulf and Caribbean Research 22:21-27.

Styles, R. 2015. Flow and turbulence over an oyster reef. Journal of Coastal Research 31:978-985.

The Nature Conservancy. 2017. Gandy's Beach shoreline protection project - final performance report. The Nature Conservancy, Delmont.

USACE. 1984. Shore protection manual. U.S. Army Corps of Engineers, Mississippi.

van der Meer, J. W., R. Briganti, B. Zanuttigh, and B. Wang. 2005. Wave transmission and reflection at low-crested structures: design formulae, oblique wave attack and spectral change. Coastal Engineering 52:915-929.

Webb, B. M., and R. J. Allen. 2015. Wave transmission through artificial reef breakwaters. Coastal Structures and Solutions to Coastal Disasters. ASCE.

Whitman, E. R., and M. A. Reidenbach. 2012. Benthic flow environments affect recruitment of Crassostrea virginica larvae to an intertidal oyster reef. Marine Ecology Progress Series 463:177-191.

Wiberg, P. L., S. R. Taube, A. E. Ferguson, M. R. Kremer, and M. A. Reidenbach. 2018. Wave attenuation by oyster reefs in shallow coastal bays. Estuaries and Coasts 42:331–347.

Woods, H., W. J. Hargis, C. H. Hershner, and P. A. M. Mason. 2005. Disappearance of the natural emergent 3-dimensional oyster reef system of the James River, Virginia 1871-1948. Journal of Shellfish Research 24:139-142.

Wright, L. D., R. A. Gammisch, and R. J. Byrne. 1990. Hydraulic roughness and mobility of three oyster-bed artificial substrate materials. Journal of Coastal Research 6:867-878.

Young, I. R., S. Zieger, and A. V. Babanin. 2011. Global trends in wind speed and wave height. Science 332:451-455.

Zhu, L., Q. Chen, H. Wang, W. Capurso, L. Niemoczynski, K. Hu, and G. Snedden. 2020. Field Observations of Wind Waves in Upper Delaware Bay with Living Shorelines. Estuaries and Coasts 43:739-755.

Table 1. Studies that have reported the percent of time a reef should be inundated for the optimal recruitment, survival and/or growth of *Crassostrea virginica*.

State	Inundation duration
North Carolina	82 – 95%[1]
North Carolina	60 – 80 %[2]
North Carolina	72 – 82 %[3]
North Carolina to Florida	52 – 84%[4]
Florida	80 – 95%[5]
Louisiana	52 – 94%[6]

[1]Fodrie et al. (2014); [2]Ridge et al. (2014); [3]Ridge et al. (2017); [4]Byers et al. (2015); [5]Solomon et al. (2014); [6]Marshall and La Peyre (2020)

Table 2. Characteristics of oyster reef living shorelines and rock sills and natural oyster reefs. Crest elevation where available is given in metres relative to NAVD88. Age is number of years at time of study. The percent of time the structures are inundated (% inundation duration) is given when (a) measured during RBR deployment; (b) calculated based on USGS gauges for deployment period; and (c) calculated based on USGS gauges from January 2017 – August 2019. For more oyster reef living shorelines characteristics refer to Appendix 1: Table S1. *Note this site is in Delaware. - data unavailable.

State/ Reef	Type	Age (yrs)	Length × Width (m)	Height (m)	Crest elevation	Tidal range (m)	% inundation duration (a)	(b)	(c)	% oysters (±SE)
NJ1	Concrete	2	6 × 1	0.65	-0.48		82.4	87.7	80.2	41.2 ± 5.2
NJ2	Shell	2	51 × 6	0.17	-0.57	1.7	68.7	74.7	75.2	0.4 ± 0.4
NJ3*	Concrete	4	2 × 1	0.53	0.01		68.7	58.6	52.6	11.3 ± 4.4
VA1	Concrete	2	16 × 0.6	0.40	0.00		67.6	53.4	50.9	6.2 ± 1.7
VA2	Shell	1	35 × 0.9	0.30	0.04	0.7	75.7	66.1	54.4	0
VA3	Concrete	1	28 × 0.85	0.30	0.01		90.9	80.0	53.5	0
FL1	Shell	8	55 × 5.25	0.64	-		38.1	-	-	2.4 ± 1.6
FL2	Shell	1	30 × 6.67	0.29	0.41	0.3	97.2	100	98	74.0 ± 3.5
FL3	Shell	2	20 × 4	0.27	0.38		75.6	100	98	34.4 ± 6.1
AL1	Shell	9	65 × 5	0.60	-0.37		100	100	99.4	-
AL2	Concrete	8	125 × 2.28	0.23	-0.24	0.4	100	100	98.3	-
AL3	Shell	8	125 × 2.64	0.31	0.17		92.9	66.7	50.4	-
LA1	Concrete	1.5	130 × 2.7	1.40	0.84		0	0	1.2	-

LA2	Concrete	1.5	178 × 5.5	1.40	0.66	0.4	0	0	4.8	-
LA3	Concrete	7	75 × 3	1.10	-0.06		63.0	81.0	84.4	-
VA1	Rock sill	2	29.4 × 2.4	0.69	0.46		30.7	8.9	9.2	1.2 ± 0.4
VA2	Rock sill	7	41.3 × 1.9	0.84	0.40	0.7	35.7	16.3	13.9	14.4 ± 4.5
VA3	Rock sill	1	51.4 × 3.6	1.02	1.03		8.9	0	0.02	0
FL1	Natural	-	47 × 7.8	0.64	-		38.1	-	-	0.4 ± 0.4
FL2	Natural	-	35 × 5.9	0.49	-	0.3	58.3	-	-	4.0 ± 2.7
FL3	Natural	-	35 × 3.1	0.33	-		64.4	-	-	2.4 ± 1.7

Figure 1. A map of the five study areas. In each study area (red dots) there were three oyster reef-control pairs, a schematic example of the wave logger (RBR) set-up for one pair is shown. The circles (oyster reef treatment) and triangles (control treatment; no reef) indicate wave sensor deployment (not to scale). For a detailed map of each area see Appendix 1: Fig. S1.

Figure 2. (a) Significant wave heights (m) at the offshore wave logger (RBR); and (b) the average depth (m) recorded during each burst at 15 oyster reef living shorelines across five locations (New Jersey/Delaware, Virginia, Florida, Alabama, Louisiana from left to right). The red lines in (b) indicate the height of the reef (m; matching scale on y-axis).

Figure 3. Comparisons of measured (y-axis) and predicted (x-axis) significant wave height (m) for (a) control (R^2=0.97); (b) oyster reef living shorelines with an inundation duration above 50% (R^2=0.97) and below 50% (R^2=0.78); (c) reefs that have an inundation duration of more than 50% and widths of less than 1 m (R^2=0.97), 2-4 m (R^2=0.97) and 5-7 m (R^2=0.96); and (d) reefs constructed of concrete (R^2=0.88) and shell (R^2=0.96). Values below the dotted line indicate a decrease in wave height. The decrease in wave height is given as a percentage on the graphs. The shaded area is the 95% confidence interval.

Figure 4. Correlation between the wave transmission coefficient (K_t) and freeboard (m) for reefs that have an inundation duration of less or greater than 50%. A wave transmission value of less than one indicates a reduction in wave height. A positive or negative freeboard value indicates the reef is emerged or submerged, respectively. The shaded area is the 95% confidence interval.

Figure 5. Comparisons of measured (y-axis) and predicted (x-axis) significant wave height (m) for (a) control (R^2=0.99), rock sill (R^2=0.94), and oyster reef living shoreline (R^2=0.98) in Virginia; (b) control (R^2=0.84), natural oyster reef (R^2=0.15), and oyster reef living shoreline (R^2=0.31) in Florida. Values below the dotted line indicate a decrease in wave height. The shaded area is the 95% confidence interval.

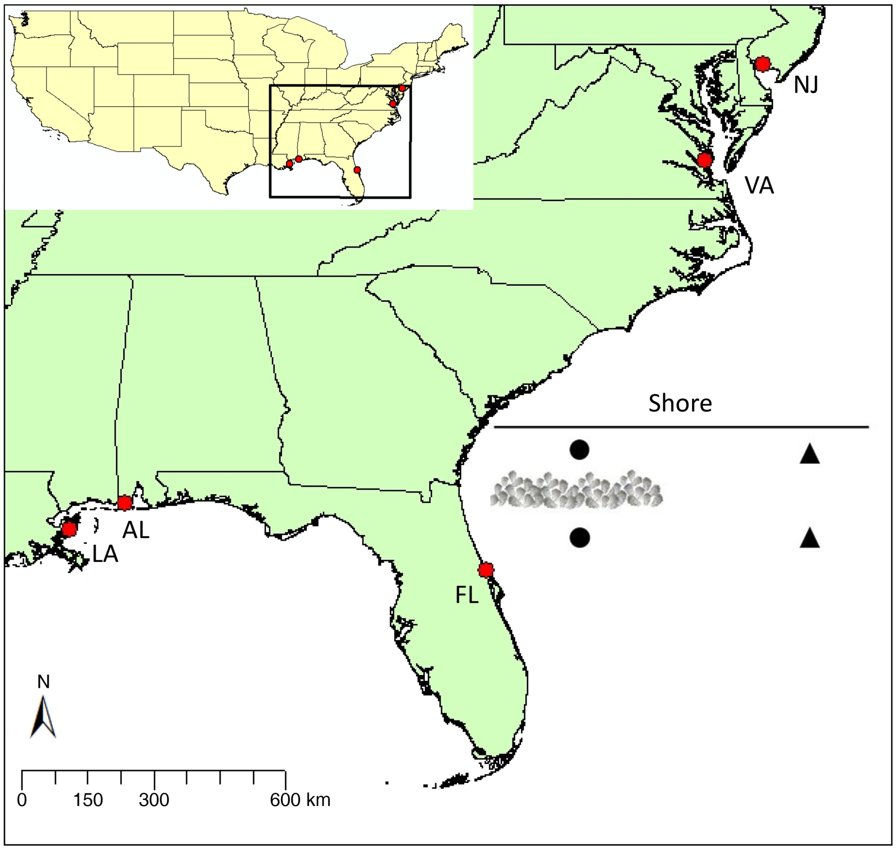

eap_2382_f1.tif

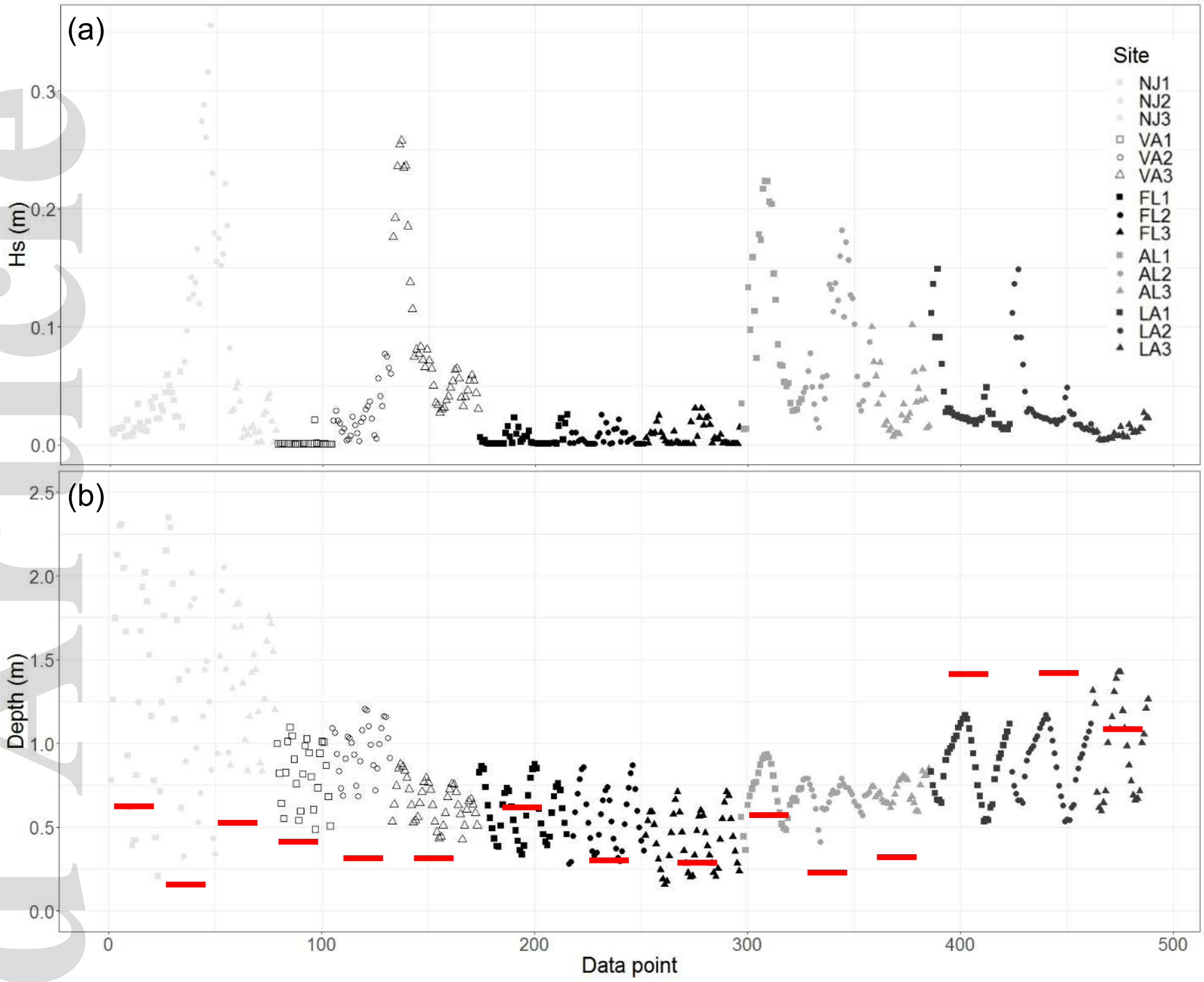
(a)
Hs (m)
0.0
0.1
0.2
0.3
Site
NJ1
NJ2
NJ3
VA1
VA2
VA3
FL1
FL2
FL3
AL1
AL2
AL3
LA1
LA2
LA3
(b)
Depth (m)
0.0
0.5
1.0
1.5
2.0
2.5
0
100
200
300
400
500
Data point

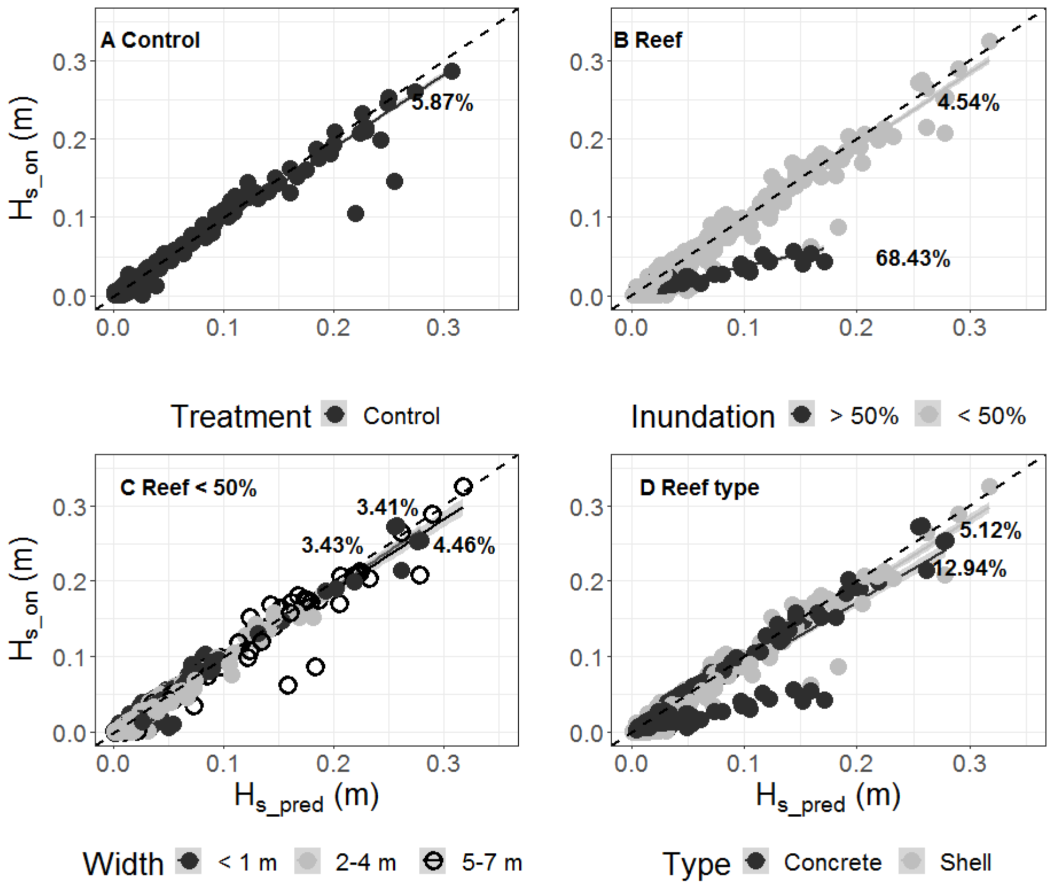

eap_2382_f3.tiff

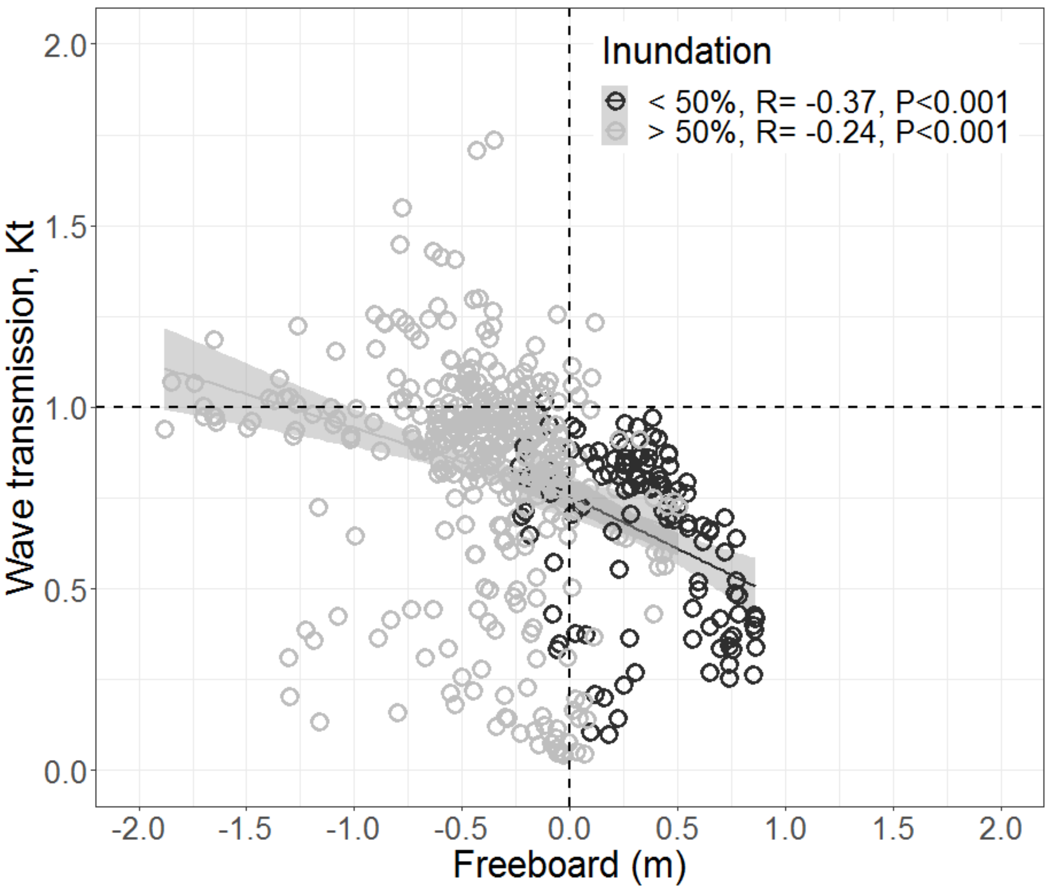

eap_2382_f4.tiff

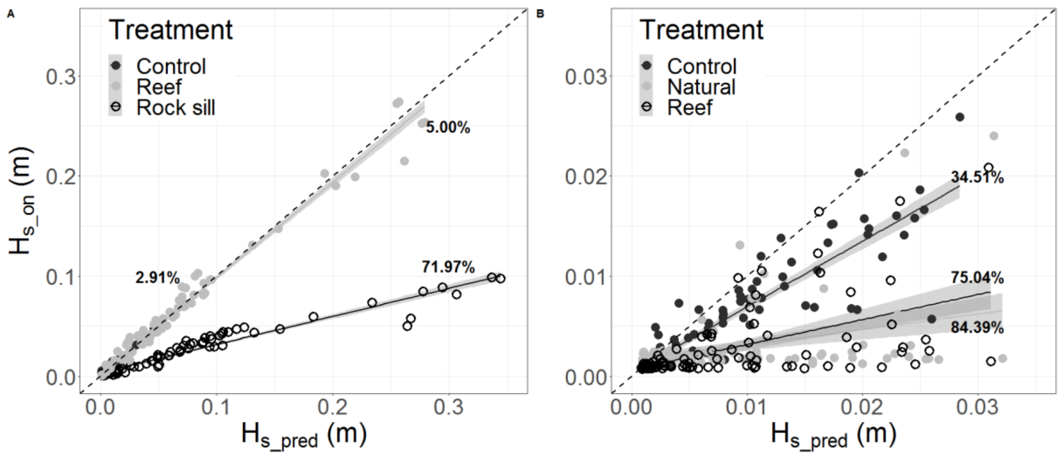

eap_2382_f5.tiff